

George H. Bryan and J. Michael Fritsch
Pennsylvania State University, University Park, PA

1. INTRODUCTION

Continuing advances in computer resources now allow researchers to simulate thunderstorms with very high resolution. For example, it is possible to simulate deep moist convection (including an entire mesoscale convective system) with grid spacing on the order of 100 m. It is natural to ask whether such high resolution is necessary, and at what point can simulations of convective processes be considered “well resolved”.

Examination of the subgrid-scale turbulence parameterizations used in cloud models provides some guidance in the debate over adequate resolution. Although not widely acknowledged, the subgrid turbulence closures in most cloud models are taken directly from large eddy simulation (LES) models. Since the subgrid turbulence schemes from LES have been included in cloud models for decades, it is important to review whether these assumptions are valid for models with the commonly used grid spacing of order 1km.

2. SUBGRID TURBULENCE

Two assumptions inherent in LES are relevant to the issue of adequate resolution:

Assumption 1: The grid spacing (Δ) is within the inertial subrange; and

Assumption 2: The scale of the phenomenon to be simulated (L) is *much larger* than the grid spacing (Δ).

The first assumption ensures that the simulation contains the largest turbulent eddies, i.e., the eddies that contain most of the kinetic energy in turbulent flows. In the inertial subrange, kinetic energy is transferred from these large eddies to much smaller eddies (of order 1 mm in size) which ultimately dissipate the energy. In LES, it is sufficient to resolve the large energy-containing eddies, while parameterizing energy transfer to subgrid scales. In other words, it is assumed that one end of the “energy cascade” is actually resolved on the model grid, and the other end can be parameterized. It has been unclear whether cloud-resolving models with $\Delta \approx 1$ km satisfy assumption #1. The most relevant study has been Droegemeier et al. (1994), who did not find clear evidence of an inertial subrange in simulations of supercell thunderstorms, even with grid spacing as small as 250 m.

Assumption 2 is a property of the closure used in LES. In the derivation of the rate of energy transfer from resolved scales to unresolved scales, it is assumed that $L \gg \Delta$. In words, a clear *scale separation* is assumed. In addition, it can be shown that assumption #2 must be satisfied in order for the flow to become

turbulent, since the Reynolds number (R_e) of the simulated flow in LES is dictated only by L and Δ , i.e.,

$$R_e \equiv \left(\frac{L}{\Delta} \right)^{\frac{4}{3}}$$

(Wyngaard 1982).

LES has been used successfully to study the planetary boundary layer (PBL) for 30 years. An evaluation of the two relevant length scales (L and Δ) used in PBL modeling may provide valuable guidance to the cloud modeling community. In boundary layer modeling with LES, $L \sim 1000$ m (the depth of the PBL), and $\Delta \sim 10$ m (a typical order-of-magnitude grid spacing). Since $L/\Delta \sim 100$, assumption 2 is satisfied, R_e is large, and the simulated flow is turbulent.

In contrast, for many cloud modeling studies, $L \sim 10$ km (a typical depth and width of a thunderstorm), and $\Delta \sim 1$ km. Since L/Δ is about 10, assumption 2 is not satisfied. Thus, the Reynolds number of the simulated flow is small, and the flow cannot become turbulent.

Considering that an L/Δ ratio of about 100 works well for LES studies of the PBL, it seems reasonable to use this relationship as guidance for the cloud modeling community. For $L \sim 10$ km, the relationship suggests that 100 m grid spacing may be necessary for the LES subgrid models to be appropriate for simulations of deep moist convection..

3. NUMERICAL SIMULATIONS

Until recently, resolution of order 100 m was not possible for simulations of deep moist convection, since it requires about 10^8 grid points for a domain that encompasses a convective system and its nearby environment. Using massively parallel computers, and a distributed memory code, we have conducted simulations of squall lines with grid spacing as small as 125 m in order to determine at what grid spacing the two assumptions are satisfied.

The numerical model used for this study is described in detail in Bryan and Fritsch (2002). The governing equations are integrated using the Runge-Kutta technique as formulated by Wicker and Skamarock (2002) for compressible models. The simulations use the Kessler microphysics scheme that includes only warm rain processes. The subgrid turbulence parameterization is similar to the one presented in Deardorff (1980).

The domain for these experiments is 300 km in the across-line direction with open boundary conditions, and 60 km in the along-line direction with periodic boundary conditions. A squall line is initiated with a north-south line thermal with a maximum perturbation of 2 K centered 1.5 km above the surface. The analytic temperature and moisture profiles of Weisman and Klemp (1982) were used to define an initially

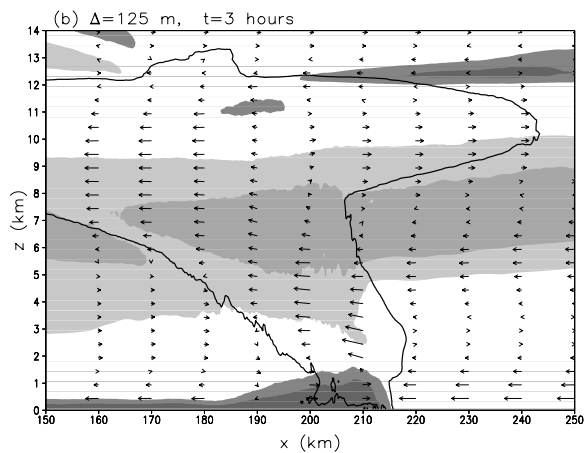
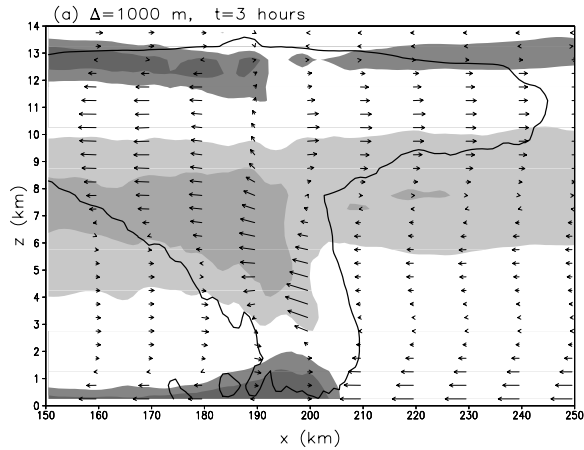


Fig. 1 Line-averaged cross section at 3 h for simulations with horizontal grid spacing of (a) 1 km, and (b) 125 m. Wind vectors are plotted every 10 km in the horizontal and every 500 m in the vertical. The thick solid line is the cloud boundary. Perturbation potential temperature is shaded, with the two darkest shades representing -2 and -4 K, and the two lighter shades representing $+2$ and $+4$ K.

horizontally homogenous environment. Simulations have been conducted using various wind profiles. Only results from a wind profile with 17.5 m s^{-1} of shear over the lowest 2.5 km are presented here.

Simulations were conducted using horizontal grid spacing of 1 km, 500 m, 250 m, and 125 m. For the 1 km simulation, the vertical grid spacing was 500 m. For all other resolutions, the vertical grid spacing was the same as the horizontal.

4. SYSTEM STRUCTURE

Details of the simulated squall line change significantly as the resolution is increased. In particular, precipitation distribution and amount, phase speed, cloud depth, mesoscale flow patterns, and stability structure are all significantly different. Line-averaged vertical cross sections (Fig. 1) illustrate some of these differences. The cross sections were created by

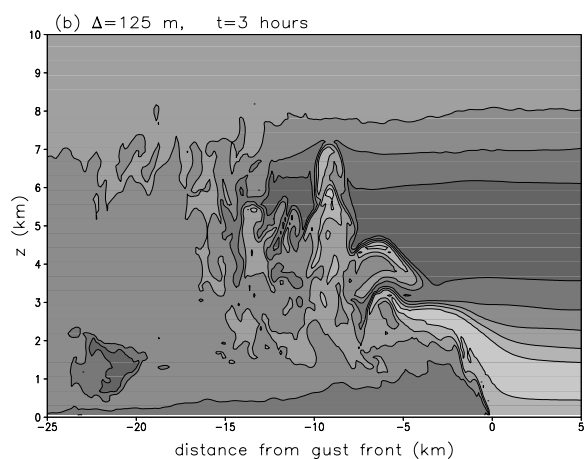
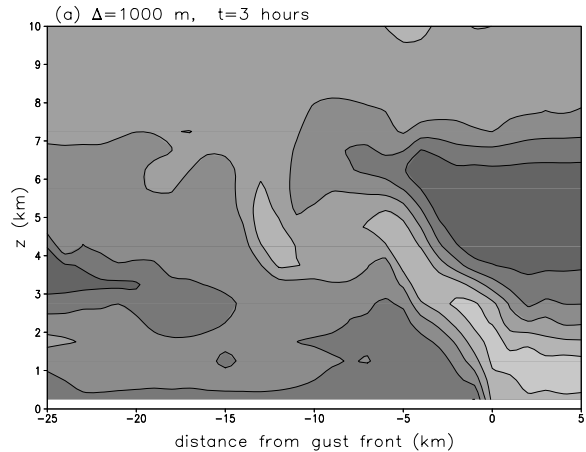


Fig. 2 Cross sections of equivalent potential temperature at 3 h for simulations with grid spacing of (a) 1 km, and (b) 125 m. Contour interval is 4 K, with the darkest shade corresponding to 326 K and the lightest shade corresponding to 342 K.

spatially averaging the instantaneous fields at 3 h in the y direction. Figure 1 presents results from the simulations with grid spacings of 1 km and 125 m.

The convective system is more upright in the 1 km simulation. Mean vertical motions at upper levels (e.g., 5-10 km above ground) are about 4 m s^{-1} in the 1 km simulation, but only about 2 m s^{-1} in the 125 m simulation (note, e.g., the upward-pointing vectors between 8-11 km in Fig 1a, as compared to the nearly horizontal vectors at the corresponding height in Fig. 1b). The magnitude of the mid-level in-cloud warm anomaly is about the same in the two simulations, with a maximum potential temperature perturbation of 5.5 K in both runs. However, this warm pool is located much closer to the leading edge of the system in the 125 m simulation. Furthermore, the subsidence-induced warm anomaly ahead of the system (below the anvil) is significantly warmer (by about 1.5 K) in the high resolution simulation. The long cold anomaly above 12 km located rearward of the maximum cloud top in the 1 km simulation is absent in the 125 m run. Horizontal flow patterns are also considerably different in the two

simulations. Most noticeable are the enhanced inflow at mid-levels (at about 6 km) and the decreased outflow near cloud top (e.g., above 10 km) in the 125 m run. Finally, the cloud boundaries are significantly different in the two simulations, with the mean cloud top being about 1 km higher in the 1 km run. *It is clear that a convergence of results has not been achieved with 1 km resolution.*

The processes that created these different patterns are being investigated. We suspect that, as argued in section 2, the different turbulent nature of the solutions is playing a primary role in creating these differences. Qualitatively, the instantaneous fields in the higher resolution are significantly more turbulent (e.g., Fig. 2). As a result, entrainment in updrafts is actually resolved in the higher resolution simulation. In contrast, Fig. 2a shows how high values of equivalent potential temperature (θ_e) can be lifted high into the squall line in a relatively laminar manner with 1 km grid spacing. The *subgrid mixing terms* might eventually diffuse away this high θ_e plume, otherwise it will ascend to the tropopause. In contrast, in the 125 m run (Fig. 2b) areas of high θ_e tend to be smaller and less coherent, as *resolved* turbulent eddies stretch and distort the θ_e field, thereby enhancing entrainment/detrainment. When considering the different nature of the overturning in these two simulations, it is not surprising to find significantly different *mesoscale* patterns of mass and momentum such as that shown in Fig. 1.

5. ENERGY SPECTRA

To determine whether the arguments made in section 2 (i.e., that 100 m grid spacing is required for the subgrid model to be appropriate), we present an analysis of the energy spectra from the four simulations. One-dimensional vertical velocity spectra were computed in the y-direction, i.e., along the convective line. Since the squall line structure varies considerably in the x-direction, it is not meaningful to average spectra in this direction, as is typically done in studies of the atmospheric boundary layer (which is statistically homogenous in *both* horizontal directions). To obtain robust energy spectra, while still averaging in a physically meaningful manner, the spectra presented here were determined by computing one spectrum per minute for 1 hour and then temporally averaging. To ensure that roughly the same area of the squall line was being analyzed at each time, the spectra were computed at the y-slice that had the highest vertical velocity variance at each time level, which at mid-levels is always along the convective region of the squall line.

The vertical velocity spectra at 5 km above ground from all four resolutions are presented in Fig. 3. The spectra are plotted from the largest scales (e.g., the 60 km along-line dimensions of the domain) to a wavelength corresponding to $6\Delta x$. It is possible to determine spectra for scales as small as $2\Delta x$, and many figures in the literature do present this information. However, we do not include data at scales smaller than $6\Delta x$ for several reasons. The numerical filter in this model (a sixth order filter) selectively damps features of

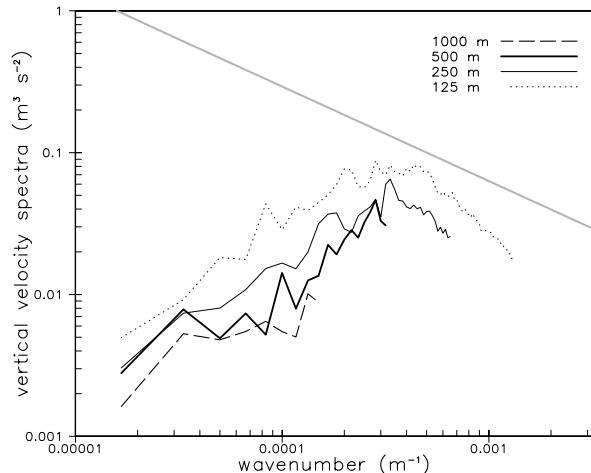


Fig. 3 One-dimensional (y-direction) vertical velocity spectra at 5 km. The spectra were computed using output every minute for 1 hr (from 120 min to 180 min). A thick gray line with slope of $\kappa^{-5/3}$ is included to illustrate behavior that is expected in an inertial subrange.

wavelength less than $6\Delta x$ (see Durran 1999). The slopes of the spectra below $6\Delta x$ are strongly affected by the intensity of the numerical filtering. Basically, it is possible to create whatever slope the user wishes below $6\Delta x$ by changing the diffusion coefficient in the model. However, the details of the spectra above $6\Delta x$ remain practically unchanged by the amount of numerical diffusion. This infers that information above $6\Delta x$ represents a physical solution while information below $6\Delta x$ represents a numerical solution that is not relevant to the issues raised in section 2.

If assumption 1 is valid, i.e., if an inertial subrange is present in the model runs, one would expect to have an energy spectrum that increases with increasing wavenumber until the scale of the large eddies, and would then decrease with increasing wavenumber with a slope of approximately $\kappa^{-5/3}$. The two highest resolution simulations (i.e., the 250 m and 125 m runs) display this qualitative behavior, while the two lower resolution runs do not. Hence, it can be concluded that *the 125 m and 250 m runs have an inertial subrange (and satisfy assumption 1), while the 500 m and 1000 m runs do not.* Not only do the coarser resolution runs not have an inertial subrange, but the 1 km simulation does not even resolve the peak in kinetic energy, which provides further evidence that LES techniques are not appropriate for grid spacings of order 1 km; energy from subgrid-scale eddies should be added to the 1 km simulation, not extracted (as LES subgrid closures do).

The spectrum from the 125 m run has a slope slightly less than $\kappa^{-5/3}$. There are several possible explanations for this unexpected result. It is possible that the grid spacing is still not small enough, and that grid spacing of order 50 m would be required. This argument is supported by the fact that assumption 2 is not satisfied; the large eddy scale (L) determined from

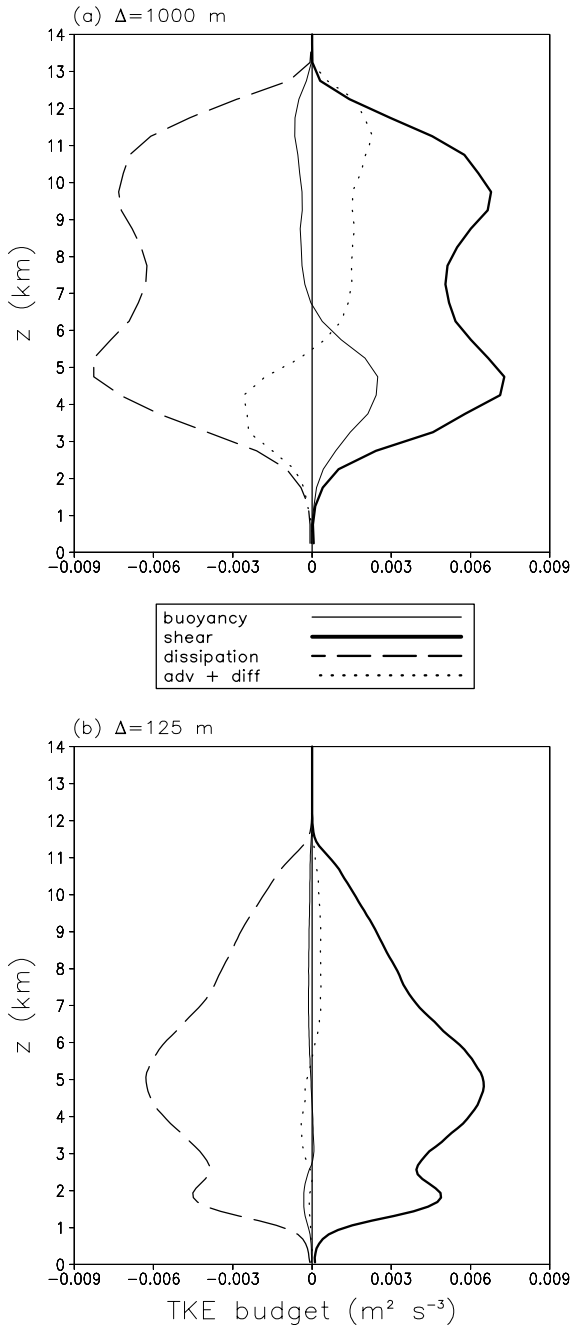


Fig. 4. Budgets of TKE, showing buoyancy contribution (thin solid), shear production (thick solid), dissipation (long dash), and the sum of advective and diffusive terms (dotted). The terms were temporally averaged from 170 to 180 min.

Fig. 3 is about 3 km, which is considerably smaller than the 10 km value used in the thought experiment at the end of section 2. This scale seems reasonable, since the largest eddies in Fig. 2b are roughly 2-3 km. A simulation with 50 m grid spacing would have an appropriately high Reynolds number for $L \sim 5$ km, which might bring the slope of the spectrum “up” to $-5/3$.

Alternatively, perhaps a $-5/3$ slope does not occur, and should not be expected, for deep moist convection with large liquid water contents. However, for lack of an alternative model of inertial subrange behavior in a moist environment, the theoretical argument of $-5/3$ will have to stand, at least for the present time.

6. BEHAVIOR OF THE SUBGRID MODEL

Analysis of the terms in the subgrid TKE equation confirms that an LES closure used in simulations with $\Delta \sim 1$ km produces behavior that is not expected in LES modeling, and is inconsistent among the various resolutions. As an example, the TKE budget averaged every time step for 10 min is presented in Fig. 4 for simulations with 1 km and 125 m grid spacing. The magnitude of the shear production term is approximately the same in the two simulations, although the shape is significantly different. At this time, we assume that the different shapes are caused primarily by the different mean flow patterns that evolve in the two simulations (e.g., Fig. 1). More relevant to this paper are the relative magnitudes of the buoyancy term, advection term, and diffusion term in the TKE budget. For example, in the 125 m run, the magnitude of the buoyancy term is only a few percent of the magnitude of the shear term. In contrast, in the 1 km run the buoyancy term is almost 1/3 of the magnitude of the shear term. In other simulations with 1 km grid spacing using weaker environmental shear profiles (not shown), the buoyancy term is actually greater than the shear term. This is clearly counter to the behavior at higher resolutions (Fig 4b), and contrary to that typically argued for LES modeling (e.g., Moeng and Wyngaard 1988).

Acknowledgements

We greatly appreciate the advice of Dr. John Wyngaard and the support of NSF grant ATM 9806309.

References

- Bryan, G. H., and J. M. Fritsch, 2002: A benchmark simulation for moist nonhydrostatic numerical models. *Mon. Wea. Rev.*, in press.
- Deardorff, J. W., 1980: Stratocumulus-capped mixed layers derived from a three-dimensional model. *Bound.-Layer Meteor.*, **18**, 495-527.
- Droegemeier, K. K., G. Bassett, and M. Xue, 1994: Very high-resolution, uniform-grid simulations of deep convection on a massively parallel computer: Implications for small-scale predictability. Preprints, *10th Conf. Numerical Weather Prediction*, Portland, OR, AMS, 376-379.
- Durrant, D. R., 1999: *Numerical Methods for Wave Equations in Geophysical Fluid Dynamics*. Springer-Verlag, 465 pp.
- Moeng, C.-H., and J. C. Wyngaard, 1988: Spectral analysis of large-eddy simulations of the convective boundary layer. *J. Atmos. Sci.*, **45**, 3573-3587.
- Weisman, M. L., and J. B. Klemp, 1982: The dependence of numerically simulated convective storms on vertical wind shear and buoyancy. *Mon. Wea. Rev.*, **110**, 504-520.
- Wicker, L. J., and W. C. Skamarock, 2002: Time splitting methods for elastic models using forward time schemes. *Mon. Wea. Rev.*, in press.
- Wyngaard, J. C., 1982: *Atmospheric Turbulence and Air Pollution Modeling*. Nieuwstadt and van Dop, Eds., 358 pp.